DOI: 10.1002/ejic.200800048

Coupling of Allenes with μ-Alkylidyne Ligands in Diiron Complexes: Synthesis of Novel Bridging Thio- and Aminobutadienylidene Complexes

Luigi Busetto,[a] Fabio Marchetti,[b] Mauro Salmi,[a] Stefano Zacchini,[a] and Valerio Zanotti*[a]

Keywords: Aminocarbyne / Thiocarbyne / Allene / Butadienylidene / C–C bond formation / Dinuclear complexes

The diiron aminocarbyne complexes $[Fe_2\{\mu\text{-}CN(Me)(R)\}(\mu\text{-}CO)(CO)_2(Cp)_2][SO_3CF_3]$ (R = Xyl, **1a**; R = 4-C_6H_4OMe, **1b**; R = Me, **1c**; Xyl = 2,6-$Me_2C_6H_3$) react with allenes of the type $CH_2{=}C{=}CR'R''$, in the presence of Me_3NO/Et_3N, to give the novel butadienylidene complexes $[Fe_2\{\mu\text{-}\eta^1{:}\eta^3\text{-}C_\alpha N(R)(Me)\text{-}C_\beta(H)C_\gamma C_\delta(R')(R'')\}(\mu\text{-}CO)(CO)(Cp)_2]$ (R = Xyl, R′ = R′′ = Me, **3a**; R = Xyl, R′ = Me, R′′ = H, **3b**; R = Xyl, R′ = CO_2Et, R′′ = H, **3c**; R = 4-C_6H_4OMe, R′ = CO_2Et, R′′ = H, **3d**; R = R′ = R′′ = Me, **3e**; R = Me, R′ = CO_2Et, R′′ = H, **3f**) in high yields. Analogously, the diiron thiocarbyne complex $[Fe_2(\mu\text{-}CSMe)(\mu\text{-}CO)(CO)_2(Cp)_2][SO_3CF_3]$ (**2**) reacts with $CH_2{=}C{=}CR'R''$, in the presence of Me_3NO/Et_3N, to afford the compounds $[Fe_2\{\mu\text{-}\eta^1{:}\eta^3\text{-}C_\alpha S(Me)C_\beta(H)C_\gamma C_\delta(R')(R'')\}(\mu\text{-}CO)(CO)(Cp)_2]$ (R′ = R′′ = Me, **4a**; R′ = CO_2Et, R′′ = H, **4b**; R′ = $SiMe_3$, R′′ = Me, **4c**). Complexes **3**–**4** exist in solution as mixtures of *cis* and *trans* isomers. Compounds **3a** and **3e**, upon treatment with HSO_3CF_3, are transformed into the corresponding vinyliminium complexes $[Fe_2\{\mu\text{-}\eta^1{:}\eta^3\text{-}C_\gamma(C_\delta HMe_2)C_\beta HC_\alpha N(R)(Me)\}(\mu\text{-}CO)(CO)(Cp)_2][SO_3CF_3]$ (R = Xyl, **5a**; R = Me, **5b**), in nearly quantitative yields. Conversely, compounds **4a**,**b** undergo methylation (by $CH_3SO_3CF_3$) at the sulfur to give the cationic complexes $[Fe_2\{\mu\text{-}\eta^1{:}\eta^3\text{-}C_\alpha(SMe_2)C_\beta(H)C_\gamma C_\delta(R')(R'')\}(\mu\text{-}CO)(CO)(Cp)_2][SO_3CF_3]$ (R′ = R′′ = Me, **7a**; R′ = CO_2Et, R′′ = H, **7b**). Protonation of **3a** is not reversible: treating **5a** with sodium hydride results in the formation of the 1-metalla-2-amino-cyclopenta-1,3-dien-5-one species $[Fe(Cp)(CO)\{CN(Me)(Xyl)CHC(CHMe_2)C(O)\}]$ (**6**). The molecular structures of *cis*-**3a**, *cis*-**4b**, **5a**$[CF_3SO_3]\cdot CH_2Cl_2$ and **7a**$[CF_3SO_3]\cdot 0.5CH_2Cl_2$ have been determined by X-ray diffraction studies.

Introduction

The assembly of simple molecular units for the construction of highly complex molecules remains a major goal for synthetic chemistry.[1] Strategies based on metal-assisted combination of molecular units include the assembly of small molecules with organic fragments coordinated to two or more metal centres. These reactions take advantage of specific organic substrate activation due to multisite coordination and of reactivity patterns which are distinct from those of corresponding species in mononuclear complexes.[2] Within this field, the coupling of bridging alkylidyne (μ-CR) and alkylidene ($\mu\text{-}CR_2$) ligands with alkynes[3] and, to a lesser extent with alkenes,[4] is well known to provide excellent routes to the synthesis of bridging C_3 hydrocarbyl ligands.

A possible extension of this approach to the synthesis of bridging C_4 hydrocarbyl species should combine $\mu\text{-}C_1$ ligands with allenes. However, examples of the incorporation of allenes into bridging hydrocarbyl ligands are relatively limited,[5] in spite of the fact that cumulenes are generally more reactive than alkenes. In particular, there are few examples of coupling reactions between allenes and bridging alkylidynes and alkylidenes. These include the reactions of allenes with the μ-methylidene complexes $[NiW(\mu\text{-}CH_2)(\mu\text{-}CO)(CO)_2(Cp)(Cp^*)]$,[6] $[Ru_2(\mu\text{-}CH_2)(\mu\text{-}CO)(CO)(MeCN)(Cp_2)]$,[7] $[RhM(CO)_2(\mu\text{-}CH_2)(dppm)_2]^+$ (M = Ru, Os)[8] and $[Fe_2(\mu\text{-}CH_2)(CO)_8]$,[3e] which lead to the formation of trimethylenemethane species (Scheme 1, **I**), and the reactions of the bridging methylidyne complexes $[L_2W(\mu\text{-}CSiMe_3)]_2$ (L = Me_3SiCH_2, *i*PrO)[9] with allenes, which afford a related C_4 allylalkylidene fragment (Scheme 1, **II**).

Our interest in the transformation of bridging ligands has been concerned so far with the assembly of amino- and thiocarbyne ligands in the diiron complexes **1** and **2** with alkynes[10] and alkenes[11] (Scheme 2). The reaction of **1** with alkynes, which affords bridging vinyliminium complexes (**a**, Scheme 2), simply consists of the alkyne insertion in the metal–carbyne bond. On the other hand, the incorporation of olefins in the bridging carbyne ligands (**b**,**c**, Scheme 2) follows a more complex sequence and requires olefin deprotonation. All of the reactions are regio- and stereocontrolled. The peculiar character of the bridging C_3 ligands formed in these assembly reactions is due to the pres-

[a] Dipartimento di Chimica Fisica e Inorganica, Università di Bologna,
Viale Risorgimento 4, 40136 Bologna, Italy
E-mail: valerio.zanotti@unibo.it
[b] Dipartimento di Chimica e Chimica Industriale, Università di Pisa,
Via Risorgimento 35, 56126 Pisa, Italy

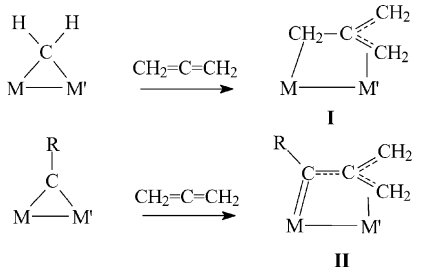

Scheme 1.

ence of heteroatoms (N or S) derived from the amino- and thiocarbyne precursors, which exert a relevant influence on the properties and reactivity of the complexes.[12]

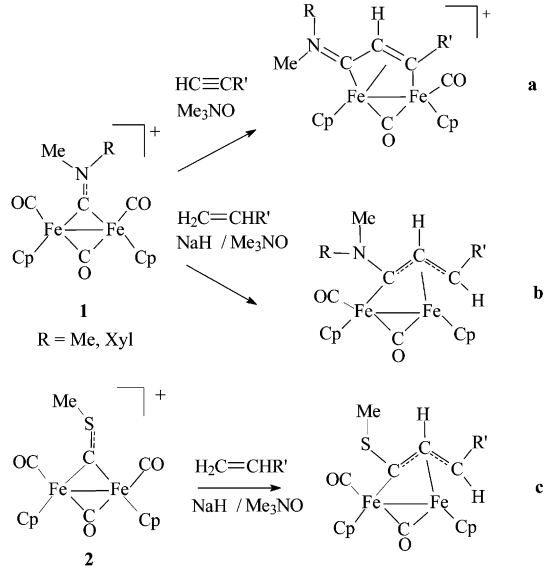

Scheme 2.

Herein we report on the reactions of the diiron μ-carbyne complexes **1** and **2** with allenes. More specifically, the purpose of our research was to determine whether or not C_4 hydrocarbyl-bridged complexes could be generated by the coupling of allenes with bridging methylidyne ligands in **1** and **2**.

Results and Discussion

The diiron aminocarbyne complexes **1a**–**c** react in THF solution with allenes, in the presence of Me_3NO and Et_3N, to afford the complexes **3a**–**f** in 70–80% yields (Scheme 3).

Compounds **3a**–**f** have been purified by chromatography on alumina and characterized by IR and NMR spectroscopy, as well as by elemental analysis. Moreover, the X-ray structure of *cis*-**3a** has been determined (Figure 1 and Table 1). The molecule is composed of a *cis*-[Fe_2(μ-CO)(CO)(Cp)$_2$] core, to which is coordinated an allenylidene [μ-

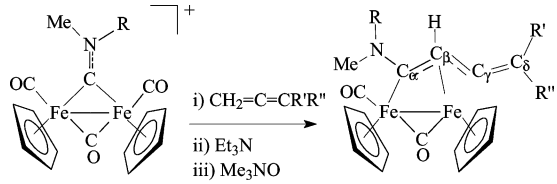

	R	R'	R''	
1a	Xyl	Me	Me	**3a**
1a	Xyl	Me	H	**3b**
1a	Xyl	CO_2Et	H	**3c**
1b	4-C_6H_4OMe	CO_2Et	H	**3d**
1c	Me	Me	Me	**3e**
1c	Me	CO_2Et	H	**3f**

Scheme 3.

η^1:η^3-$C_\alpha N(Xyl)(Me)C_\beta(H)C_\gamma C_\delta(Me)_2$] ligand. The latter can be described by using three different resonance forms (Scheme 4). The fact that all three C(13), C(14) and C(15) carbon atoms (corresponding to C_α, C_β and C_γ, respectively) are coordinated to Fe(1) [Fe(1)–C(13) 2.0648(17) Å, Fe(1)–C(14) 2.0452(17) Å, Fe(1)–C(15) 1.9647(17) Å] with relatively similar bond lengths and both C(13)–C(14) [1.431(2) Å] and C(14)–C(15) [1.407(2) Å] bonds display some π-character is in agreement with the allyl-like coordination displayed in (**A**). At the same time, the Fe(1)–C(15) bond length [1.9647(17) Å] is sensibly shorter than those of Fe(1)–C(13) [2.0648(17) Å] and Fe(1)–C(14) [2.0452(17) Å], which are almost equal; this suggests some contribution from the 1-amino-1,3-butadienylidene form (**C**). Finally, the fact that the C(14)–C(15) bond length [1.407(2) Å] is shorter than that of C(13)–C(14) [1.431(2) Å] indicates that even the aminoallenyl alkylidene form (**B**) must be considered. In agreement with all of the three structures **A**–**C**, the C(15)–C(16) interaction [1.317(3) Å] is almost a pure double bond, whereas the C(13)–N(1) bond [1.395(2) Å] is quite elongated, which suggests a limited π-interaction. All these considerations point to the fact that the coordination of such an unsaturated ligand to a bimetallic frame results in a highly delocalized and complex electronic structure which cannot be described in an unequivocal way. On the other hand, this complex system of σ- and π-interactions is probably the origin of the stabilization of the highly unsaturated organic fragments by bridging coordination.

The spectroscopic data reveal that, in solution, **3a**–**d** consist of a mixture of *cis* and *trans* isomers (*cis* and *trans* refer to the mutual positions of the Cp ligands with respect to the Fe–Fe bond). Similar *cis*-*trans* isomeric mixtures were previously observed in the complexes obtained by alkene–aminocarbyne coupling (**b**, Scheme 2).[11b] These complexes were found to undergo rearrangements of the configuration of the ancillary Cp and CO ligands (*cis*-*trans* isomerization) to better respond to changes in the steric demand of the bridging organic frame.

The IR spectra of **3a**–**d** in CH_2Cl_2 solution display two absorptions for the terminal CO ligand, in agreement with the presence of the two isomers (1946 and 1921 cm^{-1} for

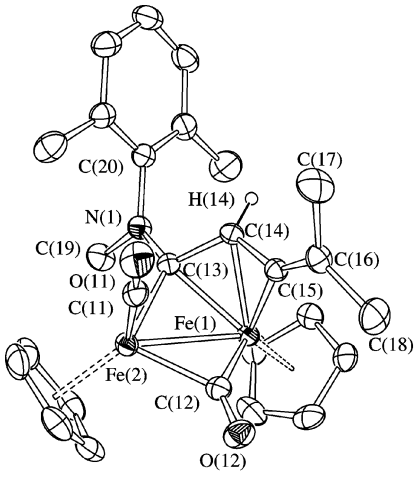

Figure 1. ORTEP drawing of $[Fe_2\{\mu\text{-}\eta^1\text{:}\eta^3\text{-}C_\alpha N(Xyl)(Me)C_\beta(H)C_\gamma C_\delta(Me)_2\}(\mu\text{-}CO)(CO)(Cp)_2]$ (*cis*-**3a**) [all H atoms, except H(14), have been omitted for clarity]. Thermal ellipsoids are shown at the 30% probability level.

Table 1. Selected bond lengths [Å] and angles [°] for $[Fe_2\{\mu\text{-}\eta^1\text{:}\eta^3\text{-}C_\alpha N(Xyl)(Me)C_\beta(H)C_\gamma C_\delta(Me)_2\}(\mu\text{-}CO)(CO)(Cp)_2]$, *cis*-**3a**.

Fe(1)–Fe(2)	2.5595(4)	C(11)–O(11)	1.153(2)
Fe(1)–C(12)	1.8702(18)	C(12)–O(12)	1.182(2)
Fe(2)–C(12)	1.9537(19)	C(13)–C(14)	1.431(2)
Fe(2)–C(11)	1.745(2)	C(14)–C(15)	1.407(2)
Fe(1)–C(13)	2.0648(17)	C(15)–C(16)	1.317(3)
Fe(2)–C(13)	2.0032(17)	C(13)–N(1)	1.395(2)
Fe(1)–C(14)	2.0452(17)	N(1)–C(19)	1.449(2)
Fe(1)–C(15)	1.9647(17)	N(1)–C(20)	1.440(2)
Fe(2)–C(13)–Fe(1)	77.96(6)	C(15)–C(16)–C(18)	123.21(19)
C(14)–C(13)–Fe(2)	117.16(12)	C(15)–C(16)–C(17)	120.96(19)
C(15)–C(14)–C(13)	120.66(16)	C(18)–C(16)–C(17)	115.78(19)
C(14)–C(15)–Fe(1)	72.57(10)	C(13)–N(1)–C(20)	120.82(14)
C(16)–C(15)–C(14)	141.06(18)	C(13)–N(1)–C(19)	123.88(15)
C(16)–C(15)–Fe(1)	145.96(15)	C(20)–N(1)–C(19)	115.04(15)

cis-**3a** and *trans*-**3a**, respectively), while one absorption (at ca. 1770 cm^{-1}) accounts for the bridging carbonyl of both isomers.

The NMR spectra show two sets of resonances. NOE investigations allow the assignment of the resonances to each isomer: indeed a significant NOE effect is detected between the Cp resonances in the case of the *cis* configuration, but not for the *trans* isomer. In spite of the fact that **3a** exhibits a *cis* configuration in the solid state, the *trans* isomers generally prevail in solution, and **3e**–**f** have been observed exclusively as *trans* isomers. Moreover, the composition of the isomeric mixture changes upon heating at reflux temperature in toluene, with conversion of *cis* into *trans*.

Besides *cis* and *trans* isomers, no other isomeric forms were observed. Indeed, the reactions with $CH_2{=}C{=}C(H)CO_2Me$ should, in theory, produce two regioisomers dependent on which of the two terminal allene carbon atoms forms the C–C bond with the μ-aminocarbyne. Conversely, the observed carbyne–allene coupling reactions are regioselective, and C–C bond formation exclusively involves the CH_2 end of the allene unit.

Notably, complexes **3a** and **3e**, obtained from dimethylallene, show distinct resonances in both the ^1H and ^{13}C NMR spectra for the two methyl groups bound to the terminal C_δ carbon of the bridging frame. This indicates that, at room temperature, there is no exchange between these groups and the bridging C_4 chain is tightly connected to the metal centres. By contrast, the *N*-methyl groups of **3e**–**f** give rise to a single resonance in both the ^1H and ^{13}C NMR spectra, and their equivalence is attributable to the loss of double bond character in the C_α–N interaction.

Finally, ^{13}C NMR spectra evidence the resonances due to C_γ and C_δ (δ = 158.9 and 118.6 ppm, respectively, for *trans*-**3a**), in the range typical of olefin carbons, as well as the C_α resonance (δ = 203.5 ppm for *trans*-**3a**), which suggests a partial aminocarbene character.

Some aspects concerning the reactions of complexes of type **1** with allenes should be pointed out. First, the reaction outcome is different from the insertion through the secondary carbon of the allene, reported in Scheme 1. By contrast, the assembly of **1** with allenes is the result of an allenyl addition at the μ-alkylidyne. Therefore it implies a deprotonation step, and the C–C bond formation involves the terminal carbon of the cumulene. It should be remarked that no reaction takes place between **1a**–**c**, allenes and Me_3NO in the absence of NEt_3 (or a different base like NaH). Thus, the coupling of **1** with allenes rather resembles the corresponding reaction with alkenes (**b**, Scheme 2), which occurs under very similar conditions.

A second observation is that, besides the deprotonation, a further requirement is the removal of a CO ligand in order to create a vacant coordination site. Most of the coupling reactions involving bridging ligands and olefins or alkynes that were mentioned in the introduction proceed only in the presence of labile ligands (acetonitrile) or under photolytic conditions. The reason for this is that preliminary coordination of the unsaturated molecules to one metal centre is

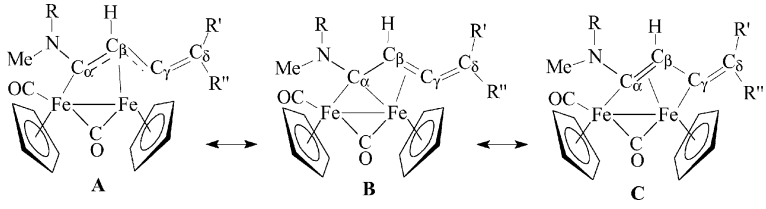

Scheme 4.

necessary to promote an intramolecular coupling between ligands. This might also be the case for the reaction of **1** with allenes. The removal of a CO ligand from **1**, accomplished upon treatment with Me_3NO, is presumably crucial in allowing coordination of the cumulene at one Fe atom in the very initial step of the reaction sequence. Thus, the observed assembling should be the result of an intramolecular coupling rather than of a direct nucleophilic allenyl attack at the bridging alkylidyne ligand. Theoretical studies indicate that the μ-alkylidyne–allene coupling involving the complex $[L_2W(\mu\text{-}CSiMe_3)]_2$[9] (Scheme 1) proceeds through the formation of an allene adduct.[13] Likewise, the reactions of the diiridium complexes $[Ir_2(CH_3)(CO)(\mu\text{-}CO)(dppm)][SO_3CF_3]$ with allenes have been shown to occur by initial η^2-allene coordination followed by intramolecular rearrangements.[14] In spite of these considerations, our attempts to detect and isolate possible η^2-allene intermediates have been unsuccessful. Our efforts included: i) low temperature reaction conditions (–40 °C), ii) the reaction of **1a** with $Me_2C{=}C{=}CMe_2$, which does not contain removable hydrogen atoms and iii) the creation of coordinative unsaturation by chloride abstraction from $[Fe_2\{\mu\text{-}CN(Me)(Xyl)\}(\mu\text{-}CO)(CO)(Cl)(Cp)_2]$ upon treatment with $AgSO_3CF_3$.

Then, investigations were extended to the thiocarbyne complex $[Fe_2\{\mu\text{-}CS(Me)\}(\mu\text{-}CO)(CO)_2(Cp)_2][SO_3CF_3]$ (**2**) in order to compare the reactivity of the thio- and aminoalkylidyne ligands and evidence the possible influence of the heteroatom (S or N). The reactions of **2** with allenes ($H_2C{=}C{=}CR'R''$), under analogous conditions to those described for the aminocarbyne complexes, result in the formation of the neutral complexes **4a**–**c** (Scheme 5), which have been purified by chromatography on alumina and characterized by spectroscopy.

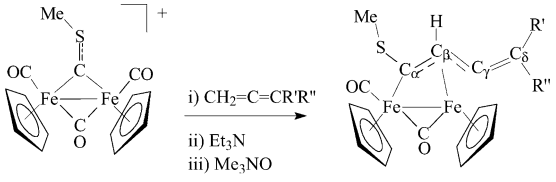

	R'	R''	
2	Me	Me	**4a**
	CO_2Et	H	**4b**
	$SiMe_3$	Me	**4c**

Scheme 5.

In addition, the molecular structure of *cis*-**4b** has been determined by X-ray diffraction (Figure 2 and Table 2). This structure is very similar to that previously described for *cis*-**3a**, apart from the different substituents on C(13) and C(16) (corresponding to C_α and C_δ). Also in this case, the $[Fe_2(\mu\text{-}CO)(CO)(Cp)_2]$ core possesses a *cis* geometry, and the coordination of the $[\mu\text{-}\eta^1{:}\eta^3\text{-}C_\alpha S(Me)C_\beta(H)\text{-}C_\gamma C_\delta(H)(CO_2Et)]$ can be described by resonance forms analogous to those depicted in Scheme 4, even though the different nature of the substituents present on C(13) and C(16) makes their relative weights different. In particular, the C(13)–C(14) [1.369(9) Å] and C(14)–C(15) [1.381(9) Å] bond lengths are inverted compared to those in *cis*-**3a** [1.431(2) Å and 1.407(2), respectively], which is more in agreement with the 1-thio-1,3-butadienylidene form (**C**) and with an allyl-like coordination (**A**). More importantly, the Fe(1)–C(15) interaction [1.906(6) Å] is considerably shorter than those of Fe(1)–C(13) [2.003(7) Å] and Fe(1)–C(14) [2.036(7) Å]; this indicates that the corresponding interactions can be more appropriately described as being nearly of σ-character for Fe(1)–C(15), whereas C(13) and C(14) are π-bonded in an olefinic fashion to Fe(1). Therefore, the bonding structure of *cis*-**4b** can be very well described by the 1-thio-1,3-butadienylidene form (**C**). It is very difficult to say whether the slightly different bonding situations in *cis*-**3a** and *cis*-**4b** are due to substitution at C(13) (amino vs. thio), or to the different groups present on C(16) (electron donating in *cis*-**3a** vs. electron withdrawing in *cis*-**4b**), or to both of them. Nonetheless, it is possible to conclude that the coordination of these unsaturated C_4 carbon chains to the $[Fe_2(\mu\text{-}CO)(CO)(Cp)_2]$ core is very flexible and sensitive to minor variations in the electronic properties even of groups not directly coordinated to the metal framework.

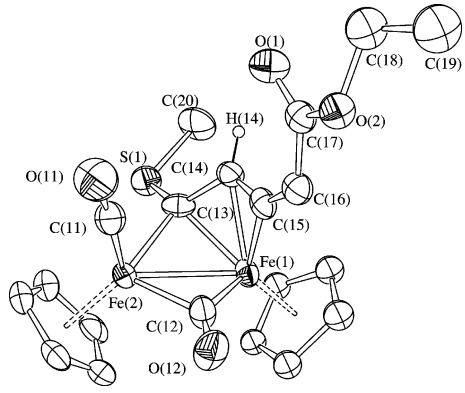

Figure 2. ORTEP drawing of $[Fe_2\{\mu\text{-}\eta^1{:}\eta^3\text{-}C_\alpha S(Me)C_\beta(H)\text{-}C_\gamma C_\delta(H)(CO_2Et)\}(\mu\text{-}CO)(CO)(Cp)_2]$ (*cis*-**4b**) [all H atoms, except H(14), have been omitted for clarity]. Only the main images of the disordered Cp ligand bonded to Fe(2) and the OEt group bonded to C(17) are drawn. Thermal ellipsoids are shown at the 30% probability level.

The similarity between complexes of type **3** and **4** is reflected in their spectroscopic properties, which are also similar (see Exp. Sect.). In particular, compounds **4a** and **4b** can be compared to **3a** and **3c**, respectively, in that they are identical except for having the SMe group in place of the NMe(Xyl) substituent. Like **3a**–**d**, complexes **4a**,**b** exist in solution as *cis* and *trans* isomers; however, the isomeric composition is different and the *cis* isomers prevail in complexes **4**. In particular, *trans* to *cis* conversion is observed upon heating at reflux temperature in THF, which is opposite to what is found in the case of type **3** complexes. These results are consistent with the *cis*/*trans* isomeric compositions observed in the complexes obtained by coupling of olefins with **1** and **2**, respectively (Scheme 2).[11]

Table 2. Selected bond lengths [Å] and angles [°] for $[Fe_2\{\mu\text{-}\eta^1\text{:}\eta^3\text{-}C_\alpha S(Me)C_\beta(H)C_\gamma C_\delta(H)(CO_2Et)\}(\mu\text{-}CO)(CO)(Cp)_2]$, *cis*-**4b**.

Fe(1)–Fe(2)	2.5221(10)	C(11)–O(11)	1.133(9)
Fe(1)–C(12)	1.872(7)	C(12)–O(12)	1.174(8)
Fe(2)–C(12)	1.950(7)	C(13)–C(14)	1.369(9)
Fe(2)–C(11)	1.753(8)	C(14)–C(15)	1.381(9)
Fe(1)–C(13)	2.003(7)	C(15)–C(16)	1.360(9)
Fe(2)–C(13)	2.002(7)	C(13)–S(1)	1.771(6)
Fe(1)–C(14)	2.036(7)	S(1)–C(20)	1.788(8)
Fe(1)–C(15)	1.906(6)	C(16)–C(17)	1.409(10)
O(1)–C(17)	1.217(8)	C(17)–O(2)	1.365(10)
Fe(2)–C(13)–Fe(1)	78.0(2)	C(15)–C(16)–C(17)	121.7(7)
C(14)–C(13)–Fe(2)	121.5(5)	O(1)–C(17)–O(2)	121.0(7)
C(15)–C(14)–C(13)	119.4(6)	O(1)–C(17)–C(16)	126.4(7)
C(14)–C(15)–Fe(1)	74.6(4)	O(2)–C(17)–C(16)	111.9(7)
C(16)–C(15)–C(14)	142.6(7)	C(17)–O(2)–C(18)	109.0(10)
C(16)–C(15)–Fe(1)	142.3(6)	C(13)–S(1)–C(20)	105.1(4)

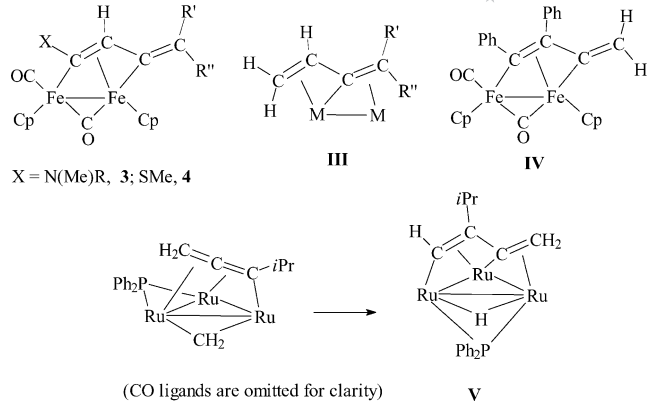

Scheme 6.

NOE investigations have been performed on complex **4c** in order to establish the orientation of the Me and $SiMe_3$ substituents on the C_δ carbon of the bridging chain. Thus, irradiation of the resonance due to $C_\delta Me$ (δ = 2.23 ppm) resulted in significant enhancements of the signals due to $C_\delta Si\mathit{Me}_3$ (δ = –0.12 ppm) and to one Cp ring (δ = 4.55 ppm). In addition, irradiation of the resonance at δ = –0.12 ppm ($C_\delta Si\mathit{Me}_3$) has revealed NOE effects with the resonances attributable to $C_\delta Me$ and $C_\beta H$ (δ = 3.87 ppm). These observations indicate that the $C_\delta Me$ group is located *anti* to $C_\beta H$, and that the more hindered $C_\delta SiMe_3$ is pointing far from the bulky Cp ligand, as expected.

Both **3** and **4** display a bridging C_4 carbon chain, which is linear (not branched) as a consequence of the fact that C–C bond formation has occurred between the μ-alkylidyne and the primary carbon of the allene. Moreover, the C_4 bridging carbon chain displays an extended π-bond as a consequence of μ-alkylidyne–allenyl coupling and of the extension of the unsaturated character of cumulene to the bridging carbyne carbon.

Analogous linear C_4 fragments bridging two adjacent metal centres are known. They include, for example, μ-η^2:η^3-2-butadienyl ligands (Scheme 6, **III**) in diruthenium[15] and diiron complexes.[16] A more appropriate comparison is with the complex $[Fe_2\{\mu\text{-}\eta^1\text{:}\eta^3\text{-}C(Ph)C(Ph)C{=}CH_2\}(\mu\text{-}CO)(CO)(Cp)_2]$[17] (Scheme 6, **IV**), which exhibits a bridging C_4 ligand very similar to that of **3** and **4**, except for the fact that it does not contain heteroatoms. The bridging C_4 frame can be described as a bridging allenylcarbene, or as a μ-η^1:η^3-butadienylidene complexes. The representations of **3**, **4** and **IV**, shown in Scheme 6, emphasize the butadienylidene nature of the bridging ligands. It should be noted that the bridging ligand in **IV**, although similar to that in **3** and **4**, is the result of a different synthetic approach in that it comes from the coupling between two C_2 units: a bridging ethylidene and a diphenylacetilene.

A further example of a bridging butadienylidene ligand is found in the triruthenium complex $[Ru_3(CO)(\mu_3\text{-}\eta^4\text{-}CH_2{=}CC(i\mathrm{Pr}){=}CH)(\mu\text{-}PPh_2)(\mu\text{-}H)]$[18] (Scheme 6, **V**).

The coordination mode of the butadienylidene ligand in **V**, which involves three metal atoms, is similar but not identical to that found in **3** and **4**. However, in this case the analogy concerns the synthetic route. As shown in Scheme 6, the C_4 ligand in **V** was obtained upon intramolecular coupling of allenyl and bridging methylidene ligands accompanied by hydrogen abstraction and coordination as a bridging hydride.[18]

The unsaturated C_4 fragment in **3** and **4** bound to multiple sites is potentially susceptible to electrophilic additions, as well as to a number of other transformations. As an example, we have investigated the reactivity of **3** and **4** with HSO_3CF_3 and $CH_3SO_3CF_3$. Compounds $[Fe_2\{\mu\text{-}\eta^1\text{:}\eta^3\text{-}C_\alpha N(R)(Me)C_\beta(H)C_\gamma C_\delta(Me)_2\}(\mu\text{-}CO)(CO)(Cp)_2]$ (R = Xyl, **3a**; R = Me, **3e**) react with HSO_3CF_3 to afford the vinyliminium complexes $[Fe_2\{\mu\text{-}\eta^1\text{:}\eta^3\text{-}C_\gamma(C_\delta HMe_2)\text{-}C_\beta HC_\alpha N(R)(Me)\}(\mu\text{-}CO)(CO)(Cp)_2][SO_3CF_3]$ (R = Xyl, **5a**; R = Me, **5b**) in nearly quantitative yields (Scheme 7).

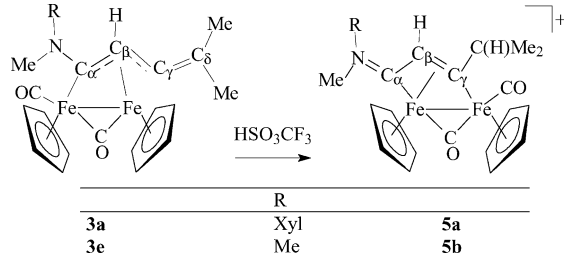

Scheme 7.

Complexes **5a**,**b** have been characterized by spectroscopy and elemental analysis. Moreover, the X-ray structure of **5a** has been determined (Figure 3 and Table 3). The cationic complex **5a** can be described as a vinyliminium cation, and all of its relevant bonding parameters perfectly parallel the ones described in the literature for analogous complexes (Scheme 2a).[10] In addition, the molecule displays a *cis* geometry for the Cp ligands, and the *E* conformation for the iminium group, as normally found for similar complexes that present a Me and a Xyl group at the iminium moiety and a hydrogen atom at C_β.

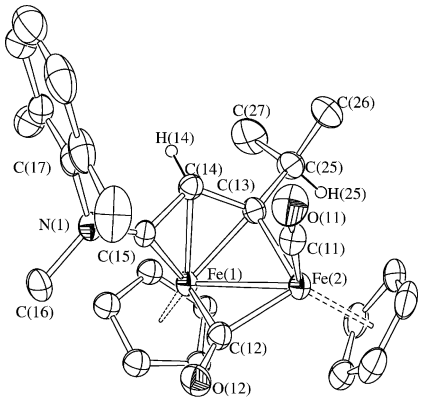

Figure 3. ORTEP drawing of $[Fe_2\{\mu\text{-}\eta^1\text{:}\eta^3\text{-}C_\gamma(C_\delta HMe_2)C_\beta HC_\alpha N(Me)(Xyl)\}(\mu\text{-}CO)(CO)(Cp)_2][SO_3CF_3]$ (**5a**) [all H atoms, except H(14) and H(25), have been omitted for clarity]. Only the main image of the disordered Cp ligand bonded to Fe(2) is drawn. Thermal ellipsoids are shown at the 30% probability level.

Table 3. Selected bond lengths [Å] and angles [°] for $[Fe_2\{\mu\text{-}\eta^1\text{:}\eta^3\text{-}C_\gamma(C_\delta HMe_2)C_\beta HC_\alpha N(Me)(Xyl)\}(\mu\text{-}CO)(CO)(Cp)_2][SO_3CF_3]$, **5a**.

Fe(1)–Fe(2)	2.5460(8)	C(11)–O(11)	1.145(6)
Fe(1)–C(12)	1.979(4)	C(12)–O(12)	1.167(5)
Fe(2)–C(12)	1.885(4)	C(13)–C(14)	1.415(6)
Fe(2)–C(11)	1.753(5)	C(14)–C(15)	1.427(6)
Fe(1)–C(13)	2.046(4)	C(15)–N(1)	1.299(5)
Fe(2)–C(13)	1.960(4)	N(1)–C(17)	1.454(6)
Fe(1)–C(14)	2.075(4)	N(1)–C(16)	1.476(6)
Fe(1)–C(15)	1.838(4)	C(13)–C(25)	1.532(6)
Fe(2)–C(13)–Fe(1)	78.89(15)	C(15)–N(1)–C(17)	123.0(4)
C(14)–C(13)–Fe(2)	121.3(3)	C(15)–N(1)–C(16)	119.8(4)
C(15)–C(14)–C(13)	118.1(4)	C(17)–N(1)–C(16)	117.1(3)
N(1)–C(15)–C(14)	132.9(4)	C(14)–C(15)–Fe(1)	77.8(2)
N(1)–C(15)–Fe(1)	147.2(3)		

The spectroscopic properties (IR and NMR spectra) of **5a**,**b** closely resemble those reported for analogous vinyliminium species.[10] The NMR spectrum of **5a** reveals the presence of two isomeric forms (*E* and *Z* isomers) that are attributable to the different orientations that the two N substituents can assume and that are due to the double-bond character of the C_α–N (iminium) interaction. As expected, the *E* isomer, in which the Xyl group points far from the Fe atom, which corresponds to the structure found in the solid, prevails in solution with an *E*/*Z* ratio of 5:1). Conversely, the NMR spectrum of **5b**, in which the N substituents are equivalent, shows one single set of resonances. NOE studies carried out on **5a**,**b** have outlined that the Cp substituents adopt the *cis* configuration. Taking into consideration that **3a** exists in solution as *cis* and *trans* isomers, and the precursor **3e** is present only in the *trans* form, the formation of **5a**,**b** must be accompanied by *trans*-*cis* isomerization. Further rearrangements involve the CO group: a terminal bound CO group is found on the Fe–Cγ metal centre instead of the Fe–C_α centre. These rearrangements of the ancillary ligand are a consequence of the "slippage" of the bridging hydrocarbyl ligand, which occurs along with the transformation into bridging vinyliminium. In fact, allyl coordination of the bridging frame shifts from one metal centre to the other and the carbon atom bridging the two metal centres changes from C_α to C_γ in **3a** and **5**.

These rearrangements evidence the flexibility and the ease by which the $Fe_2(CO)_2Cp_2$ frame accompanies the transformation of the bridging organic frame.

In order to determine whether or not the protonation reaction can be reversed upon treatment with a base, we studied the reactivity of **5a** with NaH. The reaction selectively afforded the metallacyclo complex **6**, rather than removing a proton (Scheme 8).

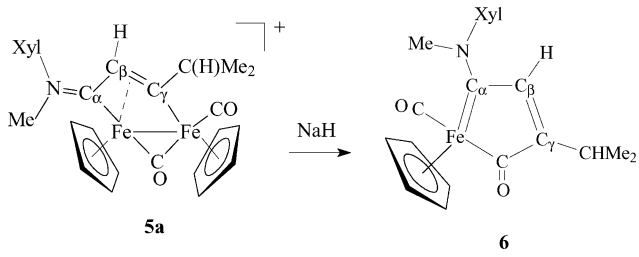

Scheme 8.

The formation of **6** is consistent with the previously reported reactions of analogous vinyliminium complexes $[Fe_2\{\mu\text{-}\eta^1\text{:}\eta^3\text{-}C_\gamma(R')C_\beta HC_\alpha N(Xyl)(Me)\}(\mu\text{-}CO)(CO)(Cp)_2][SO_3CF_3]$ (R = Me, CO_2Me, CMe_2OH) which, upon treatment with NaH, resulted in a similar fragmentation of the diiron compound and formation of the corresponding 1-metalla-2-amino-cyclopenta-1,3-dien-5-one complexes.[19]

Complex **6** has been characterized by IR and NMR spectroscopy, as well as by elemental analysis. The NMR spectra evidence the presence of *E* and *Z* isomers in about a 2:1 ratio; these are due to the different orientations that the Me and Xyl groups can assume with respect to the N–C_α bond, which exhibits some double bond character. These observations are consistent with those previously reported for the metallacyclopentadienone complexes mentioned above.[19]

By contrast with the effectiveness of the protonation reaction, we found that compounds **3** are inert towards $CH_3SO_3CF_3$. In particular, stirring a dichloromethane solution of **3a** with $CH_3SO_3CF_3$ overnight gave only trace amounts of **5a**.

Compared to **3**, the thiomethylbutadienylidene complexes **4a**,**b** show a different behaviour with respect to HSO_3CF_3 and $CH_3SO_3CF_3$. The reaction with HSO_3CF_3 does not produce any stable compound. Protonation, which presumably takes place at the S atom, is reversible, and slowly leads to the decomposition of **4a**,**b**. On the other hand, complexes **4a**,**b** undergo methylation at the S atom upon treatment with $CH_3SO_3CF_3$ in CH_2Cl_2 solution to afford the cationic complexes **7a**,**b**, which have been characterized by spectroscopy and elemental analysis (Scheme 9).

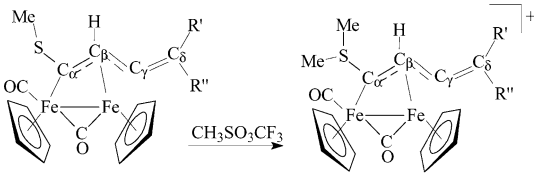

	R'	R''	
4a	Me	Me	**7a**
4b	CO_2Et	H	**7b**

Scheme 9.

Moreover, the X-ray molecular structure of **7a** has been determined (Figure 4 and Table 4). The structure of the sulfonium derivative **7a** closely resembles those of the parent neutral thio-1,3-butadienylidene complex *cis*-**4b** and the related amino compound *cis*-**3a**.

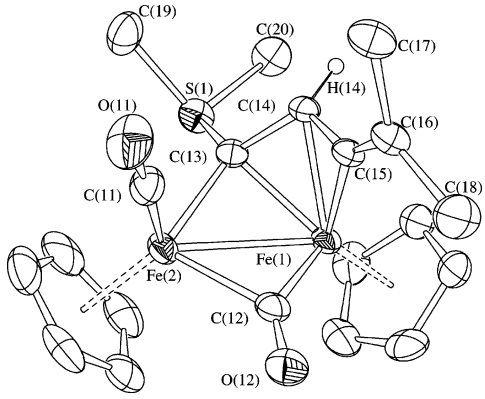

Figure 4. ORTEP drawing of $[Fe_2\{\mu\text{-}\eta^1\text{:}\eta^3\text{-}C_\alpha(SMe_2)C_\beta(H)C_\gamma C_\delta(Me)_2\}(\mu\text{-}CO)(CO)(Cp)_2][SO_3CF_3]$ (**7a**) [all H atoms, except H(14), have been omitted for clarity]. Thermal ellipsoids are shown at the 30% probability level.

Table 4. Selected bond lengths [Å] and angles [°] for $[Fe_2\{\mu\text{-}\eta^1\text{:}\eta^3\text{-}C_\alpha(SMe_2)C_\beta(H)C_\gamma C_\delta(Me)_2\}(\mu\text{-}CO)(CO)(Cp)_2][SO_3CF_3]$, **7a**.

Fe(1)–Fe(2)	2.5423(8)	C(11)–O(11)	1.141(6)
Fe(1)–C(12)	1.878(5)	C(12)–O(12)	1.171(6)
Fe(2)–C(12)	1.984(5)	C(13)–C(14)	1.417(6)
Fe(2)–C(11)	1.759(5)	C(14)–C(15)	1.398(6)
Fe(1)–C(13)	1.976(4)	C(15)–C(16)	1.323(6)
Fe(2)–C(13)	1.942(4)	C(13)–S(1)	1.773(4)
Fe(1)–C(14)	2.057(4)	S(1)–C(20)	1.791(6)
Fe(1)–C(15)	1.997(4)	S(1)–C(19)	1.798(6)
C(16)–C(17)	1.512(6)	C(16)–C(18)	1.495(7)
Fe(2)–C(13)–Fe(1)	80.91(16)	C(15)–C(16)–C(18)	122.6(4)
C(14)–C(13)–Fe(2)	123.7(3)	C(15)–C(16)–C(17)	120.0(4)
C(15)–C(14)–C(13)	116.2(4)	C(18)–C(16)–C(17)	117.3(4)
C(16)–C(15)–C(14)	143.1(4)	C(13)–S(1)–C(20)	110.1(3)
C(16)–C(15)–Fe(1)	144.6(4)	C(13)–S(1)–C(19)	101.8(3)
C(14)–C(15)–Fe(1)	72.2(2)	C(20)–S(1)–C(19)	98.8(3)

Methylation of the S atom is remarkable in that it produces only small changes in the coordination mode of the bridging ligand, in comparison to the effects generated by the protonation of **3a** and **3e**. The overall connectivity is not altered, but some bonding distances are sensibly affected. In particular, the Fe(1)–C(15) bond [1.997(4) Å] is considerably elongated compared to that of *cis*-**4b** [1.906(6) Å], whereas the Fe(1)–C(13) bond [1.976(4) Å] is shortened [2.003(7) Å in *cis*-**4b**], which suggests that **7a**,**b** are better described as bridging sulfonium-allenylalkylidene (Scheme 10, **VII**), rather than sulfonium-butadienylidene complexes (Scheme 10, **VI**).

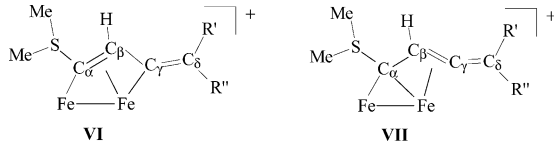

VI **VII**

Scheme 10.

In agreement with this, the C(14)–C(15) bond [1.398(6) Å] displays more pronounced π-character than the C(13)–C(14) bond [1.417(6) Å].

The spectroscopic properties of **7a**,**b** are consistent with the structural data. IR spectra (in CH_2Cl_2 solution) display the usual ν(CO) band pattern consisting of two absorptions (1988 and 1809 cm^{-1} for **7a**) that are shifted to higher frequencies by about 30 cm^{-1} compared to the parent complexes, as a consequence of the positive charge. The NMR spectra show single sets of resonances. NOE studies carried out on both **7a** and **7b** evidence that the Cp ligands also adopt the *cis* configuration in solution. The S-methyl groups give rise to a single resonance in both the ^1H and ^{13}C NMR spectra (δ = 3.75 and 39.6 ppm, respectively, for **7b**), which indicates their equivalence. Major features of the ^{13}C NMR spectra are given by resonances attributable to C_α, C_β, C_γ and C_δ, which fall, in the case of **7a**, at 159.4, 59.6, 181.0 and 114.5, respectively.

Methylation at the S atom in bridging thioalkylidene complexes of the type $[Fe_2\{\mu\text{-}C(SMe)(X)\}(\mu\text{-}CO)(CO)_2(Cp)_2]$ (X = H, CN) is well documented.[20] The formation of the corresponding bridging sulfonium-alkylidene complexes $[Fe_2\{\mu\text{-}C(SMe_2)(X)\}(\mu\text{-}CO)(CO)_2(Cp)_2][SO_3CF_3]$ has been exploited to obtain a variety of bridging alkylidene complexes by SMe_2 displacement by nucleophiles including amines, alcohols, thiols, phosphanes and carbon nucleophiles.[21] Displacement of the SMe_2 unit from the bridging ligand has also been attempted for **7a**,**b**, but without success. Indeed, compounds **7a**,**b** were unreactive with respect to $NaBH_4$ or NBu_4CN in THF at room temperature, and no replacement of the SMe_2 group by hydride or cyanide was observed.

Conclusions

Allene incorporation into bridging amino- and thioalkylidyne complexes follows a general behaviour and is not affected by the nature of the heteroatom (N or S) on the bridging ligand. The coupling reaction requires proton removal from the allene and the presence of a vacant coordination site on one iron centre, in order to allow preliminary

allene coordination. Allenyl–alkylidyne coupling generates a bridging C_4 frame, which can be described as a thio- or amino-$\eta^1\eta^3$-butadienylidene ligand or, alternatively, as a bridging thio- or aminoallenylalkylidene ligand. The whole of these representations accounts for the extended π-bond in the bridging frame, which supports multisite coordination and allows for the addition of electrophilic reagents such as HSO_3CF_3 and $CH_3SO_3CF_3$. The reactivity of the butadienylidene ligand is influenced by the nature of the heteroatom substituents (N or S). Thus, methylation of the bridging thiobutadienylidene complexes occurs selectively at the S atom, to generate the corresponding sulfonium derivatives. By contrast, protonation of the aminobutadienylidene complexes takes place at the terminal carbon of the C_4 chain and transforms the bridging frame into a stable vinyliminium ligand. Once again, these reactions evidence the role of the rather flexible dinuclear frame $Fe_2(CO)_2Cp_2$ in supporting transformations of the bridging ligand, in that they are accompanied and sustained by proper changes in the coordination mode or in the configuration of the ancillary ligands (*cis-trans* isomerizations).

Experimental Section

General: All reactions were routinely carried out under a nitrogen atmosphere using standard Schlenk techniques. Solvents were distilled immediately before use under nitrogen from appropriate drying agents. Chromatography separations were carried out on columns of deactivated alumina (4% w/w water). Glassware was oven-dried before use. Infrared spectra were recorded at 298 K with a Perkin–Elmer Spectrum 2000 FTIR spectrophotometer and elemental analyses were performed on a ThermoQuest Flash 1112 Series EA Instrument. All NMR measurements were performed at 298 K with a Mercury Plus 400 instrument. The chemical shifts for ^1H and ^{13}C were referenced to internal TMS. The spectra were fully assigned with DEPT experiments and ^1H–^{13}C correlation through gs-HSQC and gs-HMBC experiments.[22] NOE measurements were recorded using the DPFGSE-NOE sequence.[23] NMR signals due to a second (minor) isomeric form (where it has been possible to detect and/or resolve them) are italicized. All reagents were commercial products (Aldrich) of the highest purity available and used as received. $[Fe_2(CO)_4(Cp)_2]$ was purchased from Strem and used as received. Compounds **1a**, **1b**[12a], **1c**[24] and **2**[25] were prepared by published methods.

Synthesis of $[Fe_2\{\mu\text{-}\eta^1\text{:}\eta^3\text{-}C_\alpha N(R)(Me)C_\beta(H)C_\gamma C_\delta(R')(R'')\}(\mu\text{-}CO)(CO)(Cp)_2]$ (R = Xyl, R′ = R″ = Me, 3a; R = Xyl, R′ = Me, R″ = H, 3b; R = Xyl, R′ = CO_2Et, R″ = H, 3c; R = 4-C_6H_4OMe, R′ = CO_2Et, R″ = H, 3d; R = R′ = R″ = Me, 3e; R′ = CO_2Et, R″ = H, 3f): A solution of complex **1a** (205 mg, 0.330 mmol) in THF (15 mL) was treated with $H_2C{=}C{=}CMe_2$ (0.10 mL, 1.02 mmol), Et_3N (0.90 mL, 6.5 mmol) and Me_3NO (50 mg, 0.67 mmol). The mixture was stirred for 30 min, then it was filtered through alumina, and the solvent was removed under reduced pressure. Chromatography of the residue on alumina, with diethyl ether as eluent, gave a green band corresponding to **3a**. Yield 132 mg, 78%. Crystals suitable for X-ray analysis were obtained from a diethyl ether solution layered with *n*-pentane at –20 °C. $C_{27}H_{29}Fe_2NO_2$ (511.22): calcd. C 63.44, H 5.72; found C 63.51, H 5.62. IR (CH_2Cl_2): $\tilde{\nu}$ = ν(CO) 1946 (s), 1921 (vs), 1760 (s) cm^{-1}. ^1H NMR ([D$_6$]acetone): δ = 7.76–7.10 (m, 3 H, $Me_2C_6H_3$); *5.10*, *4.70*, 4.40, 4.39 (s, 10 H, Cp); 3.91, *3.88* (s, 3 H, NMe); *3.08*, 3.02 (s, 1 H, $C_\beta H$); 2.65, *2.62*, 2.44, *2.39* (s, 6 H, $Me_2C_6H_3$); 2.18, *2.01*, *1.70*, 1.31 (s, 6 H, $C_\delta Me_2$) ppm. *trans*/*cis* ratio 3:2. $^{13}C\{^1H\}$ NMR ([D$_6$]-acetone): δ = 265.1, *263.7* (μ-CO); *215.6*, 214.0 (CO); *204.5*, 203.5 (C_α); 158.9, *158.4* (C_γ); 147.8 (*ipso*-$Me_2C_6H_3$); 135.1, 134.2, 129.8, *129.6*, 129.3, *128.6*, 126.7, *126.5* ($Me_2C_6H_3$); *120.2*, 118.6 (C_δ); 88.1, *86.1*, 84.6, *83.3* (Cp); 47.7, *44.4* (NMe); *47.3*, 35.2 (C_β); 26.9, *26.0*, *21.2*, 20.6 ($C_\delta Me_2$); *19.8*, 19.4, 19.0, *18.7* ($Me_2C_6H_3$) ppm. Compounds **3b**,**c** were prepared by the same procedure described for **3a** by reacting **1a** (200 mg) with Et_3N, Me_3NO and the appropriate allene.

3b: Yield 112 mg, 70%; colour: green. $C_{26}H_{27}Fe_2NO_2$ (497.19): calcd. C 62.81, H 5.47; found C 62.88, H 5.42. IR (CH_2Cl_2): $\tilde{\nu}$ = ν(CO) 1950 (s), 1920 (vs), 1767 (s) cm^{-1}. ^1H NMR ($CDCl_3$): δ = 7.44–7.08 (m, 3 H, $Me_2C_6H_3$); *5.00*, *4.78*, 4.67, 4.40 (s, 10 H, Cp); 4.16, *4.08* (s, 1 H, $C_\delta H$); *3.89*, 3.80 (s, 3 H, NMe); 3.17 (s, 1 H, $C_\beta H$); 2.60, *2.57*, 2.38 (s, 6 H, $Me_2C_6H_3$); *2.17*, 2.08 (s, 3 H, $C_\delta Me$) ppm. *trans*/*cis* ratio 6:5. $^{13}C\{^1H\}$ NMR ($CDCl_3$): δ = 264.3, *262.1* (μ-CO); *216.0*, 214.0 (CO); *206.5*, 202.1 (C_α); 157.4, *157.2* (C_γ); 148.0 (*ipso*-$Me_2C_6H_3$); 134.8–126.3 ($Me_2C_6H_3$); 120.9 (C_δ); *87.0*, 86.9, 86.2, *84.9* (Cp); 47.7, *44.4* (NMe); 47.4 (C_β); 29.2, *27.9* ($C_\delta Me$); *20.8*, 19.6, 18.8, *17.9* ($Me_2C_6H_3$) ppm.

3c: Yield 136 mg, 76%; colour: green. $C_{28}H_{29}Fe_2NO_4$ (555.22): calcd. C 60.57, H 5.26; found C 60.56, H 5.29. IR (CH_2Cl_2): $\tilde{\nu}$ = ν(CO) 1964 (vs), *1922* (s), 1770 (s), 1729 (m), ν($C_\gamma C_\delta$) 1676 (m) cm^{-1} ppm. ^1H NMR ($CDCl_3$): δ = 7.33–7.16 (m, 3 H, $Me_2C_6H_3$); *5.95*, 5.76 (d, $^4J_{HH}$ = 2 Hz, 1 H, $C_\delta H$); 5.09, 4.68, *4.48*, *4.33* (s, 10 H, Cp); 4.00 (br., 2 H, CO_2CH_2); 3.85, *3.84* (s, 3 H, NMe); *3.26*, 3.16 (d, $^4J_{HH}$ = 2 Hz, 1 H, $C_\beta H$); 2.58, 2.40 (s, 6 H, $Me_2C_6H_3$); 1.29 (br., 3 H, $CO_2CH_2CH_3$) ppm. *cis*/*trans* ratio 2:1. $^{13}C\{^1H\}$ NMR ($CDCl_3$): δ = 266.3 (μ-CO); 216.3 (CO); 203.0 (C_α); 189.4, *189.2* (C_γ); 159.4 (CO_2Et); 146.0 (*ipso*-$Me_2C_6H_3$); 135.6–126.7 ($Me_2C_6H_3$); 111.4, *109.4* (C_δ); *88.5*, 86.0, 85.7, *84.2* (Cp); 59.2 (CO_2CH_2); 49.7, *48.8* (NMe); 47.7, *37.6* (C_β); 19.8, *19.4*, *19.0*, 18.5 ($Me_2C_6H_3$); 14.2, *13.8* ($CO_2CH_2CH_3$) ppm.

Compound **3d** was prepared by the same procedure described for **3a** by reacting **1b** (273 mg) with Et_3N, Me_3NO and $CH_2{=}C{=}CH(COOEt)$.

3d: Yield 174 mg, 71%; colour: green. $C_{27}H_{27}Fe_2NO_5$ (557.20): calcd. C 58.20, H 4.88; found C 58.25, H 4.76. IR (CH_2Cl_2): $\tilde{\nu}$ = ν(CO) 1966 (vs), 1936 (s), 1778 (s), 1729 (m) cm^{-1}. ^1H NMR ($CDCl_3$): δ = 7.67–6.90 (m, 4 H, C_6H_4OMe); 5.98, *5.88* (d, $^4J_{HH}$ = 2.2 Hz, 1 H, $C_\delta H$); 4.72, *4.66*, *4.64*, 4.55 (s, 10 H, Cp); 4.12 (s, 3 H, OMe); 4.01 (s, 3 H, NMe); 4.00 (br., 2 H, CO_2CH_2); 3.36, *3.30* (d, $^4J_{HH}$ = 2.2 Hz, 1 H, $C_\beta H$); 1.26 (br., 3 H, $CO_2CH_2CH_3$) ppm. *cis*/*trans* ratio 3:2. $^{13}C\{^1H\}$ NMR ($CDCl_3$): δ = 265.7, *263.5* (μ-CO); 215.0 (CO); *202.3*, 200.7 (C_α); 189.4, *189.2* (C_γ); 156.9 (CO_2Me); 150.0, 128.6, 127.9, 125.8, 114.9, 114.2 (C_6H_4Me); *111.8*, 110.0 (C_δ); 88.7, *86.7*, 85.2, *84.5* (Cp); 59.6, *59.5* (CO_2CH_2); 55.7, *55.6* (OMe); *47.3*, 35.2 (C_β); 43.7, *43.5* (NMe); *14.5*, 14.1 ($CO_2CH_2CH_3$) ppm.

Compound **3e**–**f** were prepared by the same procedure described for **3a** by reacting **1c** (230 mg) with Et_3N, Me_3NO and the appropriate allene.

***trans*-3e:** Yield 134 mg, 72%; colour: green. $C_{20}H_{23}Fe_2NO_2$ (421.09): calcd. C 57.05, H 5.51; found C 57.12, H 5.46. IR (CH_2Cl_2): $\tilde{\nu}$ = ν(CO) 1919 (vs), 1764 (s) cm^{-1}. ^1H NMR ($CDCl_3$): δ = 4.50, 4.23 (s, 10 H, Cp); 3.64 (s, 6 H, NMe_2); 3.45 (s, 1 H, $C_\beta H$); 2.31, 1.79 (s, 6 H, $C_\delta Me_2$) ppm. $^{13}C\{^1H\}$ NMR ($CDCl_3$): δ = 267.2 (μ-CO); 214.1 (CO); 204.1 (C_α); 159.4 (C_γ); 119.0 (C_δ); 87.7, 83.5 (Cp); 46.2 (NMe_2); 35.4 (C_β); 26.8, 21.5 ($C_\delta Me_2$) ppm.

***trans*-3f:** Yield 165 mg, 80%; colour: green. $C_{21}H_{23}Fe_2NO_4$ (465.10): calcd. C 54.23, H 4.98; found C 54.29, H 4.88. IR (CH_2Cl_2): $\tilde{\nu}$ = ν(CO) 1931 (vs), 1783 (s), 1730 (w) cm^{-1}. ^1H NMR ($CDCl_3$): δ = 6.04 (br., 1 H, $C_\delta H$); 4.52, 4.28 (s, 10 H, Cp); 3.65 (s, 6 H, NMe_2); 4.05 (br., 2 H, CO_2CH_2); 3.44 (br., 1 H, $C_\beta H$); 1.23 (br., 3 H, $CO_2CH_2CH_3$) ppm. $^{13}C\{^1H\}$ NMR ($CDCl_3$): δ = 265.5 (μ-CO); 213.1 (CO); 202.8 (C_α); 195.5 (C_γ); 163.0 (CO_2Et); 109.2 (C_δ); 88.5, 84.8 (Cp); 59.3 (CO_2CH_2); 46.3 (NMe_2); 38.0 (C_β); 14.5 ($CO_2CH_2CH_3$) ppm.

Synthesis of $[Fe_2\{\mu\text{-}\eta^1\text{:}\eta^3\text{-}C_\alpha S(Me)C_\beta(H)C_\gamma C_\delta(R')(R'')\}(\mu\text{-}CO)(CO)(Cp)_2]$ (R′ = R″ = Me, 4a; R′ = CO_2Et, R″ = H, 4b; R′ = $SiMe_3$, R″ = Me, 4c): A solution of **2** (300 mg, 0.561 mmol) in THF (20 mL) was treated with $H_2C{=}C{=}CMe_2$ (0.10 mL, 1.02 mmol), Et_3N (1.2 mL, 8.7 mmol) and Me_3NO (84 mg, 1.12 mmol). The resulting mixture was stirred for 40 min, and then was filtered through alumina. Removal of the solvent gave a residue that was chromatographed on alumina using diethyl ether as eluent. A green band was collected to afford **4a** as a green-brown powder upon solvent removal. Yield 178 mg, 75%. $C_{19}H_{20}Fe_2O_2S$ (424.12): calcd. C 53.81, H 4.75; found C 53.89, H 4.66. IR (CH_2Cl_2): $\tilde{\nu}$ = ν(CO) 1959 (vs), 1936 (s), 1781 (s) cm^{-1}. ^1H NMR ($CDCl_3$): δ = 4.87, 4.54, *4.52*, *4.25* (s, 10 H, Cp); *4.16*, 4.00 (s, 1 H, $C_\beta H$); 2.90, *2.87* (s, 3 H, SMe); *2.27*, 2.11, *1.80*, 1.65 (s, 6 H, $C_\delta Me_2$) ppm. *cis*/*trans* ratio 5:3. $^{13}C\{^1H\}$ NMR ($CDCl_3$): δ = 262.6, *261.3* (μ-CO); 212.7, *212.1* (CO); *188.4*, 188.1 (C_α); *158.0*, 155.4 (C_γ); 122.8, *120.4* (C_δ); *88.2*, 87.4, *86.3*, 84.7 (Cp); *51.3*, 50.4 (C_β); 27.1, *26.7*, *21.6*, 21.1 ($C_\delta Me_2$); *20.6*, 20.4 (SMe) ppm. Compounds **4b**,**c** were prepared by the same procedure described for **4a** by reacting **2** (300 mg) with Et_3N, Me_3NO and the appropriate allene $H_2C{=}C{=}C(R')(R'')$. Crystals of **4b** suitable for X-ray analysis were obtained from a $CDCl_3$ solution layered with *n*-pentane at –20 °C.

4b: Yield 205 mg, 78%; colour: green. $C_{20}H_{20}Fe_2O_4S$ (468.13): calcd. C 51.31, H 4.31; found C 51.36, H 4.30. IR (CH_2Cl_2): $\tilde{\nu}$ = ν(CO) 1977 (s), 1953 (vs), 1788 (s), 1709 (w) cm^{-1}. ^1H NMR ($CDCl_3$): δ = 5.92, *5.81* (d, $^4J_{HH}$ = 2.20 Hz, 1 H, $C_\delta H$); *4.95*, 4.78, *4.57*, 4.29 (s, 10 H, Cp); 4.67, *4.56* (d, $^4J_{HH}$ = 2.20 Hz, 1 H, $C_\beta H$); 4.12, *3.98* (m, 2 H, CO_2CH_2); *2.88*, 2.87 (s, 3 H, SMe); 1.20, *1.14* (m, 3 H, $CO_2CH_2CH_3$) ppm. *trans*/*cis* ratio 3:1. $^{13}C\{^1H\}$ NMR ($CDCl_3$): δ = *262.1*, 259.9 (μ-CO); 210.8, *210.3* (CO); 191.5, 190.1, *189.7*, *188.5* (C_α and C_γ); 162.5, *162.4* (CO_2Et); *111.4*, 110.2 (C_δ); 89.0, *88.0*, 87.4, *85.9* (Cp); *59.6*, 59.5 (CO_2CH_2); 54.3, *52.5* (C_β); 20.9, *20.7* (SMe); 14.4, *14.2* ($CO_2CH_2CH_3$) ppm.

***cis*-4c:** Yield 198 mg, 73%; colour: brownish green. $C_{21}H_{26}Fe_2O_2SSi$ (482.27): calcd. C 52.30, H 5.43; found C 52.32, H 5.39. IR (CH_2Cl_2): $\tilde{\nu}$ = ν(CO) 1961 (vs), 1778 (s) cm^{-1}. ^1H NMR ($CDCl_3$): δ = 4.86, 4.55 (s, 10 H, Cp); 3.87 (s, 1 H, $C_\beta H$); 2.83 (s, 3 H, SMe); 2.23 (s, 3 H, $C_\delta Me$); –0.12 (s, 9 H, $SiMe_3$) ppm. $^{13}C\{^1H\}$ NMR ($CDCl_3$): δ = 262.9 (μ-CO); 213.2 (CO); 188.3 (C_α); 168.4 (C_γ); 125.0 (C_δ); 87.8, 85.1 (Cp); 49.4 (C_β); 20.7 (SMe); 17.9 ($C_\delta Me$); –1.9 ($SiMe_3$) ppm.

Synthesis of $[Fe_2\{\mu\text{-}\eta^1\text{:}\eta^3\text{-}C_\gamma(C_\delta HMe_2)C_\beta HC_\alpha N(R)(Me)\}(\mu\text{-}CO)(CO)(Cp)_2][SO_3CF_3]$ (R = Xyl, 5a; R = Me, 5b): Compound **3a** (112 mg, 0.219 mmol) was dissolved in CH_2Cl_2 (10 mL) and treated with HSO_3CF_3 (0.025 mL, 0.283 mmol). The solution was stirred for 15 min, and then the solvent was removed under reduced pressure. Chromatography of the residue on an alumina column with CH_3OH as eluent gave a red band corresponding to **5a**. Yield 123 mg, 85%. Crystals suitable for X-ray analysis were obtained from a CH_2Cl_2 solution layered with diethyl ether at –20 °C. $C_{28}H_{30}F_3Fe_2NO_5S$ (661.29): calcd. C 50.86, H 4.57; found C 51.00, H 4.62. IR (CH_2Cl_2): $\tilde{\nu}$ = ν(CO) 2002 (vs), 1814 (s), ν(CN) 1631 (m) cm^{-1}. ^1H NMR ($CDCl_3$): δ = 7.40–6.93 (m, 3 H, $Me_2C_6H_3$); 5.41, *5.23*, 5.21, *4.82* (s, 10 H, Cp); *5.08*, 4.22 (s, 1 H, $C_\beta H$); 4.69 (m, 1 H, $CHMe_2$); 4.19, *3.93* (s, 3 H, NMe); 2.24, *1.87*, 1.75 (s, 6 H, $Me_2C_6H_3$); 1.51 (dq, $^3J_{HH}$ = 12, $^4J_{HH}$ = 6.6 Hz, 6 H, $CHMe_2$) ppm. *E*/*Z* ratio 5:1. $^{13}C\{^1H\}$ NMR ($CDCl_3$): δ = 254.0 (μ-CO); 231.5 (C_α); 210.1 (CO); 208.0 (C_γ); 145.0 (*ipso*-$Me_2C_6H_3$); 131.4, 131.1, 129.9, 129.7, 129.5 ($Me_2C_6H_3$); *92.6*, 91.8, *91.6*, 87.6 (Cp); 58.0 (C_δ); 54.9 (C_β); 45.9 (NMe); 31.1 ($CHMe_2$); 18.0, *17.5*, 16.7 ($Me_2C_6H_3$). Complex **5b** was prepared by the same procedure described for **5a** by reacting **3e** (128 mg) with HSO_3CF_3 ppm.

5b: Yield 139 mg, 80%; colour: light green. $C_{21}H_{24}F_3Fe_2NO_5S$ (571.17): calcd. C 44.16, H 4.24; found C 44.17, H 4.20. IR (CH_2Cl_2): $\tilde{\nu}$ = ν(CO) 1988 (vs), 1806 (s), ν(CN) 1682 (w) cm^{-1}. ^1H NMR ($CDCl_3$): δ = 5.13, 5.08 (s, 10 H, Cp); 4.98 (br. s, 1 H, $C_\beta H$); 4.92 (m, 1 H, $CHMe_2$); 3.85, 3.26 (s, 6 H, NMe); 1.90 (dq, $^3J_{HH}$ = 12, $^4J_{HH}$ = 7.7 Hz, 6 H, $CHMe_2$) ppm. $^{13}C\{^1H\}$ NMR ($CDCl_3$): δ = 255.2 (μ-CO); 224.2 (C_α); 209.3 (CO); 208.5 (C_γ); 91.2, 87.7 (Cp); 56.7 (C_β); 52.0 (C_δ); 51.7, 45.1 (NMe); 33.3 ($CHMe_2$) ppm.

Synthesis of $[Fe(CO)(Cp)\{C_\alpha N(Me)(Xyl)C_\beta HC_\gamma(C_\delta HMe_2)C(O)\}]$ (6): A solution of **5a** (123 mg, 0.186 mmol) in THF (10 mL) was treated with NaH (44 mg, 1.91 mmol). The mixture was stirred for 30 min, and then it was filtered through an alumina pad. Removal of the solvent and chromatography of the residue on an alumina column with THF as eluent gave a brown band corresponding to **6**. Yield 55 mg, 75%. $C_{22}H_{25}FeNO_2$ (391.28): calcd. C 67.53, H 6.44; found C 67.61, H 6.39. IR (CH_2Cl_2): $\tilde{\nu}$ = ν(CO) 1917 (vs), 1591 (m), ν(C_αN) 1620 (m) cm^{-1}. ^1H NMR ($CDCl_3$): δ = 7.34–7.13 (m, 3 H, $Me_2C_6H_3$); 6.43 (s, 1 H, $C_\beta H$); 4.61 (s, 5 H, Cp); 3.82 (s, 3 H, NMe); 2.70 (m, 1 H, $C_\delta H$); 2.20, 2.08 (s, 6 H, $Me_2C_6H_3$); 0.84 (dq, $^3J_{HH}$ = 10.6, $^4J_{HH}$ = 6.6 Hz, 6 H, $C_\delta Me_2$) ppm. *E*/*Z* ratio 2:1. $^{13}C\{^1H\}$ NMR ($CDCl_3$): δ = 272.6 (C=O); 264.0 (C_α); 222.5 (CO); 173.6 (C_γ); 148.6 (C_β); 145.3 (*ipso*-$Me_2C_6H_3$); 132.6, 132.1, 129.4, 128.9, 128.7 ($Me_2C_6H_3$); 84.9 (Cp); 48.7 (NMe); 37.1 (C_δ); 21.5 ($C_\delta Me_2$); 17.3, 17.2 ($Me_2C_6H_3$) ppm.

Synthesis of $[Fe_2\{\mu\text{-}\eta^1\text{:}\eta^3\text{-}C_\alpha(SMe_2)C_\beta(H)C_\gamma C_\delta(R')(R'')\}(\mu\text{-}CO)(CO)(Cp)_2][SO_3CF_3]$ (R′ = R″ = Me, 7a; R′ = CO_2Et, R″ = H, 7b): $CH_3SO_3CF_3$ (0.03 mL, 0.27 mmol) was added to a solution of **4a** (100 mg, 0.236 mmol) in CH_2Cl_2 (12 mL). The mixture was stirred for 2 h, and then it was chromatographed on an alumina column. Elution with a 1:1 mixture of THF and methanol gave a green band corresponding to **7a**. Yield 111 mg, 80%. Crystals suitable for X-ray analysis were obtained from a dichloromethane solution layered with diethyl ether at –20 °C. $C_{21}H_{23}F_3Fe_2O_5S_2$ (588.22): calcd. C 42.88, H 3.94; found C 42.96, H 4.04. IR (CH_2Cl_2): $\tilde{\nu}$ = ν(CO) 1988 (vs), 1809 (s) cm^{-1}. ^1H NMR ($CDCl_3$): δ = 4.86, 4.70 (s, 10 H, Cp); 4.18 (s, 1 H, $C_\beta H$); 3.35 (s, 6 H, SMe); 1.95, 1.50 (s, 6 H, $C_\delta Me_2$) ppm. $^{13}C\{^1H\}$ NMR ($CDCl_3$): δ = 251.9 (μ-CO); 209.6 (CO); 155.8 (C_α); 151.2 (C_δ); 127.1 (C_γ); 86.9, 84.3 (Cp); 55.7 (C_β); 38.7 (SMe); 27.2, 20.7 ($C_\delta Me_2$) ppm.

Complex **7b** was prepared by the same procedure described for **7a** by reacting **4b** (109 mg) with $CH_3SO_3CF_3$.

7b: Yield 107 mg, 73%; colour: green. $C_{22}H_{23}F_3Fe_2O_7S_2$ (632.23): calcd. C 41.79, H 3.67; found C 41.85, H 3.59. IR (CH_2Cl_2): $\tilde{\nu}$ = ν(CO) 2002 (vs), 1806 (s), 1701 (m) cm^{-1}. ^1H NMR ($CDCl_3$): δ = 5.86 (br. s, 1 H, $C_\delta H$); 5.21, 5.03 (s, 10 H, Cp); 4.88 (br. s, 1 H, $C_\beta H$); 3.93 (m, 2 H, CO_2CH_2); 3.75 (s, 6 H, SMe); 1.06 (m, 3 H, $CO_2CH_2CH_3$) ppm. $^{13}C\{^1H\}$ NMR ($CDCl_3$): δ = 252.9 (μ-CO); 207.8 (CO); 181.0 (C_γ); 159.4 (C_α); 161.9 (CO_2Et); 114.5 (C_δ); 88.2, 86.4 (Cp); 60.2 (CO_2CH_2); 59.6 (C_β); 39.6 (SMe); 14.2 ($CO_2CH_2CH_3$) ppm.

X-ray Crystallography: Crystal data for *cis*-**3a**, *cis*-**4b**, **5a**$[CF_3SO_3]\cdot CH_2Cl_2$ and **7a**$[CF_3SO_3]\cdot 0.5CH_2Cl_2$ were collected at room tem-

Table 5. Crystal data and experimental details for *cis*-**3a**, *cis*-**4b**, **5a**$[CF_3SO_3]\cdot CH_2Cl_2$ and **7a**$[CF_3SO_3]\cdot 0.5CH_2Cl_2$.

Complex	*cis*-**3a**	*cis*-**4b**	**5a**$[CF_3SO_3]\cdot CH_2Cl_2$	**7a**$[CF_3SO_3]\cdot 0.5CH_2Cl_2$
Formula	$C_{27}H_{29}Fe_2NO_2$	$C_{20}H_{20}Fe_2O_4S$	$C_{29}H_{32}Cl_2F_3Fe_2NO_5S$	$C_{21.5}H_{24}ClF_3Fe_2O_5S_2$
FW	511.21	468.12	746.22	630.68
T [K]	296(2)	195(2)	295(2)	295(2)
λ [Å]	0.71073	0.71073	0.71073	0.71073
Crystal system	monoclinic	orthorhombic	monoclinic	monoclinic
Space group	$P2_1/c$	$P2_12_12_1$	$P2_1/c$	$P2_1/c$
a [Å]	9.0799(4)	8.7598(6)	10.3736(6)	9.8512(6)
b [Å]	29.2031(12)	12.4318(9)	18.7998(11)	26.8978(16)
c [Å]	9.6739(4)	18.1162(13)	16.9447(10)	9.8626(3)
β [°]	110.3590(10)	90	101.5620(10)	92.9460(10)
Cell volume [Å^3]	2404.90(18)	1972.9(2)	3237.5(3)	2609.9(3)
Z	4	4	4	4
D_c [g cm^{-3}]	1.412	1.576	1.531	1.605
μ [mm^{-1}]	1.230	1.599	1.181	1.426
$F(000)$	1064	960	1528	1284
Crystal size [mm]	$0.21\times0.17\times0.13$	$0.24\times0.18\times0.14$	$0.23\times0.19\times0.13$	$0.24\times0.20\times0.15$
θ limits [°]	2.35–27.10	1.99–25.99	1.64–27.00	1.51–27.00
Reflections collected	20747	20386	35640	28837
Independent reflections	5317 [R_{int} = 0.0301]	3880 [R_{int} = 0.0419]	7061 [R_{int} = 0.0473]	5701 [R_{int} = 0.0340]
Data/restraints/parameters	5317/11/297	3880/117/245	7061/166/393	5701/128/330
Goodness of fit on F^2	1.026	1.059	1.039	1.052
R_1 [$I>2\sigma(I)$]	0.0288	0.0549	0.0606	0.0579
wR_2 (all data)	0.0747	0.1412	0.1903	0.1935
Largest diff. peak and hole [e Å^{-3}]	0.261/–0.187	0.933/–0.382	0.862/–0.736	1.352/–0.645

perature with a Bruker AXS SMART 2000 CCD diffractometer using Mo-K_α radiation. Intensity data were measured over full diffraction spheres using 0.3° wide ω scans, with a crystal-to-detector distance of 5.2 cm. Cell dimensions and orientation matrixes were initially determined from least-squares refinements on reflections measured in 3 sets of 20 exposures collected in three different ω regions and eventually refined against all reflections. The SMART software[26] was used for collecting frames of data, indexing reflections and determining lattice parameters. The collected frames were then processed for integration by the SAINT software, and empirical absorption corrections were applied with SADABS.[27] The structure was solved by direct methods and refined by full-matrix least-squares based on all data using F^2.[28] The crystal data are listed in Table 5. Non-H atoms were refined anisotropically, unless otherwise stated. H atoms were placed in calculated positions, except for H(14) in *cis*-**3a**, *cis*-**4b** and **7a**$[CF_3SO_3]\cdot 0.5CH_2Cl_2$ and H(14) and H(25) in **5a**$[CF_3SO_3]\cdot CH_2Cl_2$, which were located in the Fourier map and refined isotropically with a thermal parameter 20% greater than that of the attached carbon. One Cp ligand and the OEt group in *cis*-**4b**, one Cp ligand and the CH_2Cl_2 molecule in **5a**$[CF_3SO_3]\cdot CH_2Cl_2$ and the CH_2Cl_2 molecule in **7a**$[CF_3SO_3]\cdot 0.5CH_2Cl_2$ are disordered. Disordered atomic positions were split and refined isotropically using similar distances and U restraints and one occupancy parameter per disordered group, apart from the CH_2Cl_2 molecule in **7a**$[CF_3SO_3]\cdot 0.5CH_2Cl_2$ for which the two disordered images are related by an inversion centre; in this case, an occupancy factor of 0.5 was assigned to the independent image of the molecule and then it was refined anisotropically. Similar U restraints were applied to all C and O atoms in *cis*-**4b**, all C atoms in **5a**$[CF_3SO_3]\cdot CH_2Cl_2$ and all C and F atoms in **7a**$[CF_3SO_3]\cdot 0.5CH_2Cl_2$. The *cis*-**4b** crystals appeared to be racemically twinned with a refined Flack parameter of 0.49(4).[29]

CCDC-673762 (for **3a**), -673763 (for **4b**), -673764 (for **5a**$[CF_3SO_3]\cdot CH_2Cl_2$) and -673765 (for **7a**$[CF_3SO_3]\cdot 0.5CH_2Cl_2$) contain the supplementary crystallographic data for this paper. These data can be obtained free of charge from The Cambridge Crystallographic Data Centre via www.ccdc.cam.ac.uk/data_request/cif.

Acknowledgments

We thank the Ministero dell'Università e della Ricerca Scientifica e Tecnologica (MURST) (project: "New strategies for the control of reactions: interactions of molecular fragments with metallic sites in unconventional species") and the University of Bologna for financial support.

[1] A. de Meijere, H. Hopf, *Chem. Rev.* **2006**, *106*, 4785–4786.
[2] V. Ritleng, M. J. Chetcuti, *Chem. Rev.* **2007**, *107*, 797–858.
[3] Selected examples: a) A. F. Dyke, S. A. R. Knox, P. J. Naish, G. E. Taylor, *J. Chem. Soc., Chem. Commun.* **1980**, 803–805; b) P. Q. Adams, D. L. Davies, A. F. Dyke, S. A. R. Knox, K. A. Mead, P. Woodward, *J. Chem. Soc., Chem. Commun.* **1983**, 222–224; c) R. E. Colburn, D. L. Davies, A. F. Dyke, S. A. R. Knox, K. A. Mead, A. G. Orpen, *J. Chem. Soc., Dalton Trans.* **1989**, 1799–1805; d) S. A. R. Knox, *J. Organomet. Chem.* **1990**, *400*, 255–272; e) C. E. Sumner Jr., J. A. Collier, R. Pettit, *Organometallics* **1982**, *1*, 1350–1360; f) C. P. Casey, L. K. Woo, P. J. Fagan, R. E. Palermo, B. R. Adams, *Organometallics* **1987**, *6*, 447–454; g) M. H. Chisholm, J. A. Heppert, J. C. Huffman, *J. Am. Chem. Soc.* **1984**, *106*, 1151–1153; h) M. H. Chisholm, C. D. Ontiveros, *Polyhedron* **1988**, *7*, 1015–1021; i) M. Cowie, *Can. J. Chem.* **2005**, *83*, 1043–1055.
[4] a) A. F. Dyke, J. E. Guerchais, S. A. R. Knox, J. Roue, R. L. Short, G. E. Taylor, P. Woodward, *J. Chem. Soc., Chem. Commun.* **1981**, 537–538; b) C. P. Casey, P. J. Fagan, *J. Am. Chem. Soc.* **1982**, *104*, 4950–4951; c) C. P. Casey, M. W. Meszaros, S. R. Marder, P. J. Fagan, *J. Am. Chem. Soc.* **1984**, *106*, 3680–3681; d) C. P. Casey, M. W. Meszaros, P. J. Fagan, R. K. Bly, R. E. Colborn, *J. Am. Chem. Soc.* **1986**, *108*, 4053–4059; e) C. P. Casey, M. W. Meszaros, S. R. Marder, R. K. Bly, P. J. Fagan, *Organometallics* **1986**, *5*, 1873–1879; f) J. A. K. Howard, S. A. R. Knox, N. J. Terrill, M. I. Yates, *J. Chem. Soc., Chem.*

Commun. **1989**, 640–642; g) J. Levisalles, F. Rose-Munch, H. Rudler, J. C. Daran, Y. Dromzee, Y. Jeannin, *J. Chem. Soc., Chem. Commun.* **1981**, 152–154.
[5] a) D. Lentz, S. Willemsen, *J. Organomet. Chem.* **2002**, *641*, 215–219; b) M. H. Chisholm, C. M. Cook, J. C. Huffman, W. E. Streib, *Organometallics* **1993**, *12*, 2677–2685; c) G. Conole, K. Henrick, M. McPartlin, A. D. Horton, M. J. Mays, E. Sappa, *J. Chem. Soc., Dalton Trans.* **1990**, 2367–2374; d) S. A. R. Knox, D. A. V. Morton, A. G. Orpen, M. L. Turner, *Inorg. Chim. Acta* **1994**, *220*, 201–214.
[6] M. J. Chetcuti, P. E. Fanwick, B. E. Grant, *Organometallics* **1991**, *10*, 3003–3004.
[7] M. J. Fildes, S. A. R. Knox, A. G. Orpen, M. L. Turner, M. I. Yates, *J. Chem. Soc., Chem. Commun.* **1989**, 1680–1682.
[8] A. Chokshi, B. D. Rowsell, S. J. Trepanier, M. J. Ferguson, M. Cowie, *Organometallics* **2004**, *23*, 4759–4770.
[9] M. H. Chisholm, K. Folting, J. A. Heppert, W. E. Streib, *J. Chem. Soc., Chem. Commun.* **1985**, 1755–1757.
[10] a) V. G. Albano, L. Busetto, F. Marchetti, M. Monari, S. Zacchini, V. Zanotti, *Organometallics* **2003**, *22*, 1326–1331; b) V. G. Albano, L. Busetto, F. Marchetti, M. Monari, S. Zacchini, V. Zanotti, *J. Organomet. Chem.* **2004**, *689*, 528–538.
[11] a) L. Busetto, F. Marchetti, M. Salmi, S. Zacchini, V. Zanotti, *J. Organomet. Chem.* **2007**, *692*, 2245–2252; b) L. Busetto, F. Marchetti, M. Salmi, S. Zacchini, V. Zanotti, *J. Organomet. Chem.* **2008**, *693*, 57–67.
[12] a) L. Busetto, F. Marchetti, S. Zacchini, V. Zanotti, *Organometallics* **2006**, *25*, 4808–4816; b) L. Busetto, F. Marchetti, S. Zacchini, V. Zanotti, *Organometallics* **2007**, *26*, 3577–3584; c) L. Busetto, F. Marchetti, S. Zacchini, V. Zanotti, *Eur. J. Inorg. Chem.* **2007**, *13*, 1799–1807.
[13] E. D. Jemmis, B. V. Prasad, *Polyhedron* **1988**, *7*, 871–879.
[14] D. Ristic-Petrovic, D. J. Anderson, J. R. Torkelson, M. J. Ferguson, R. McDonald, M. Cowie, *Organometallics* **2005**, *24*, 3711–3724.
[15] J. N. L. Dennett, S. A. R. Knox, J. P. H. Charmant, A. L. Gillon, A. G. Orpen, *Inorg. Chim. Acta* **2003**, *354*, 29–40.
[16] S. M. Breckenridge, S. A. MacLaughlin, N. J. Taylor, A. J. Carty, *J. Chem. Soc., Chem. Commun.* **1991**, 1718–1720.
[17] C. P. Casey, W. H. Miles, P. J. Fagan, K. J. Haller, *Organometallics* **1985**, *4*, 559–563.
[18] D. Nucciarone, N. J. Taylor, A. J. Carty, *Organometallics* **1984**, *3*, 177–179.
[19] L. Busetto, F. Marchetti, S. Zacchini, V. Zanotti, *Organometallics* **2005**, *24*, 2297–2306.
[20] a) V. G. Albano, S. Bordoni, D. Braga, L. Busetto, A. Palazzi, V. Zanotti, *Angew. Chem. Int. Ed. Engl.* **1991**, *30*, 847–849; b) S. Bordoni, F. Mazza, V. Zanotti, *Inorg. Chim. Acta* **1994**, *223*, 31–35.
[21] L. Busetto, V. Zanotti, *J. Organomet. Chem.* **2005**, *690*, 5430–5440.
[22] W. Wilker, D. Leibfritz, R. Kerssebaum, W. Beimel, *Magn. Reson. Chem.* **1993**, *31*, 287–292.
[23] K. Stott, J. Stonehouse, J. Keeler, T. L. Hwang, A. J. Shaka, *J. Am. Chem. Soc.* **1995**, *117*, 4199–4200.
[24] G. Cox, C. Dowling, A. R. Manning, P. McArdle, D. Cunningham, *J. Organomet. Chem.* **1992**, *438*, 143–158.
[25] M. H. Quick, R. Angelici, *J. Inorg. Chem.* **1981**, *20*, 1123–1130.
[26] *SMART & SAINT* Software Reference Manuals, Version 5.051, Bruker Analytical X-ray Instruments Inc., Madison, Wi, **1998**.
[27] G. M. Sheldrick, *SADABS*, Program for empirical absorption correction, University of Göttingen, Germany, **1996**.
[28] G. M. Sheldrick, *SHELX97*, Program for crystal structure determination, University of Göttingen, Germany, **1997**.
[29] H. D. Flack, *Acta Crystallogr.* **1983**, *3*, 876–881.

Received: January 15, 2008
Published Online: April 9, 2008

